Renewable and Sustainable Energy Reviews 31 (2014) 563–574

Contents lists available at ScienceDirect

Renewable and Sustainable Energy Reviews

journal homepage: www.elsevier.com/locate/rser

A review of the CIE general sky classification approaches

Danny H.W. Li*, T.C. Chau, Kevin K.W. Wan

Building Energy Research Group, Department of Civil and Architectural Engineering, City University of Hong Kong, Tat Chee Avenue, Kowloon, Hong Kong SAR, China

ARTICLE INFO

Article history:
Received 29 November 2012
Received in revised form
8 November 2013
Accepted 19 December 2013
Available online 21 January 2014

Keywords:
CIE Standard Skies
Sky distribution
Vertical sky component
Climatic parameters
Sky classification

ABSTRACT

Recently, the International Commission on Illumination (CIE) has adopted a range of 15 standard sky distributions representing the whole probable spectrum of actual skies in the world. Each sky standard has its own well-defined sky luminance pattern which can be conveniently used to calculate the sky radiance and luminance for a given sky patch and the solar irradiance and daylight illuminance on inclined surfaces facing various orientations. The crucial issues are whether the skies could be correctly identified. This paper presents the work on the classification of the CIE Standard General Skies using various climatic parameters and indices. Meteorological variables namely luminance distribution for the whole sky including zenith luminance, global, direct-beam and sky-diffuse illuminance on a horizontal surface and vertical sky illuminance, and horizontal and vertical solar irradiance data are adopted for analysis. The results demonstrate that there are a number of appropriate climatic parameters for sky classification and the selection depends on their availability, accuracy and sensitivity. The approaches could contribute to the estimation of solar irradiance and daylight illuminance which are essential to the renewable and sustainable developments and energy-efficient building designs.

Contents

1. Introduction

Solar radiation and natural light data are essential to architects, engineers and scientists for renewable and sustainable developments including active solar energy applications [1,2] passive

* Corresponding author. Tel.: +852 34427063; fax: +852 34420427.
E-mail address: bcdanny@cityu.edu.hk (D.H.W. Li).

1364-0321/$ - see front matter
http://dx.doi.org/10.1016/j.rser.2013.12.018

Nomenclature

a, *b*, *c*, *d* and *e*	adjustable coefficients
a_v	luminous ideal extinction
B_v	direct-beam daylight illuminance (lux)
B_{VT}	direct-beam illuminance on a vertical surface (lux)
D_v	horizontal sky-diffuse illuminance (lux)
D_{VT}	sky-diffuse illuminance on a vertical surface (lux)
E_v	extraterrestrial illuminance (lux)
G_v	horizontal global illuminance (lux)
G_{VT}	daylight illuminance incident on a vertical surface (lux)
I_{VT}	sky-diffuse solar irradiance on a vertical plane (W/m²)
L	sky luminance (cd/m²)
L_{mea}	measured sky point luminance (cd/m²)
l_{pred}	predicted sky point luminance in relative form
L_z	zenith luminance (cd/m²)
m_v	optical air mass
N	the number of reading
R_{VT}	ground-reflected illuminance on a vertical surface (lux)
T_v	luminous turbidity
V_{fs}	sky illuminance on a vertical surface facing to the sun (lux)
V_{os}	sky illuminance on a vertical surface facing to opposite of the sun (lux)
Z	zenith angle of a sky element (rad)
Z_s	zenith angle of the sun (rad)
α	altitude angle of a sky element (rad)
α_s	solar altitude (rad)
ρ	ground reflectance
ϕ_{Nr}	azimuth angle of the surface normal (rad)
ϕ	azimuth angle of a sky element (rad)
χ	scattering angle (degrees)

Abbreviation

CIE	International Commission on Illumination
NR	normalization ratio
RMSE	root-mean-square error
SSLD	standard sky luminance distribution
VCR	vertical component ratio
VSC	vertical sky component

energy-efficient building designs [3–6], test reference year databases generation [7,8], climatology studies [9–11] and pollution assessments [12]. An accurate estimation of the available solar radiation and daylight is to acquire, not just the total amount of radiation and light coming from the sky, but also the radiance and luminance patterns over the sky vault [13,14]. The solar radiance and sky luminance distributions are influenced by many factors, including solar position, turbidity and pollution content of the atmosphere and cloud type and amount, which cause numerous interactions of sunlight and skylight [15]. Generally, sky conditions can be interpreted into overcast, partly cloudy and clear skies. Sky conditions of the same category would have similar solar radiance and sky luminance distributions and the corresponding climatic parameters would be within certain ranges [16]. Recently, the International Commission on Illumination (CIE) has adopted a range of 15 standard skies [17] proposed by Kittler et al. [18] as an international standard sky model. A number of researchers have reported that the 15 CIE standard skies provide a good overall framework for representing the actual sky conditions and cover the whole probable spectrum of skies found in nature [19–23]. Each CIE General Standard Sky is well-defined by sky luminance pattern which is the straightforward approach for sky classification [24]. In many locations of the world, the basic sky luminance data are not readily available [25]. In interpreting sky conditions, meteorological data are initially used as weighting factors to show the degree of sky clearness but different researchers adopted different climatic indices with various ranges [26–30]. The choice depends on the availability, accuracy and sensitivity of these meteorological variables [31]. Currently, a number of climatic parameters including sky luminance distribution, ratio of zenith luminance to horizontal sky-diffuse illuminance (L_Z/D_V), ratio of horizontal sky-diffuse illuminance to extraterrestrial illuminance (D_V/E_V), ratio of horizontal global illuminance to extraterrestrial illuminance (G_V/E_V), and vertical sky component (VSC) were proposed for differentiating the 15 CIE General Standard Skies [32–34]. This paper reviews and evaluates the performance of individual sky classification processes. Modifications of some sky identification procedures are elaborated. A comparative analysis of the performance for various sky classification approaches is reported. Relevant climatic elements under individual standard skies are examined and implications discussed.

2. CIE standard skies

The 15 CIE General Standard Skies are referred to Standard Sky Luminance Distribution (SSLD). Each sky standard is the product of a gradation function and a scattering indicatrix function [17]. The gradation refers to the sky luminance that varies smoothly between horizon and zenith. In general, higher sky luminance is at the zenith under overcast skies but opposite trend appears for clear skies with larger luminance towards the horizon. The scattering indicatrix represents the direct sunlight scattering in the atmosphere. For a cloudless sky, peak luminance is near to the solar position and drops swiftly with the distance from the sun [35]. Under overcast conditions, skies are either independent of or slight brightening towards the sun. The mathematical expressions for the relative sky luminance (l_S), relative graduation $\varphi(Z)/\varphi(0°)$ and relative scattering indicatrix $f(\chi)/f(Z_S)$ are given as follows:

$$l_S = \frac{L}{L_Z} = \frac{f(\chi)\varphi(Z)}{f(Z_S)\varphi(0°)} \tag{1}$$

$$\frac{\varphi(Z)}{\varphi(0°)} = \frac{1+a\ \exp(b/\cos Z)}{1+a\ \exp\ b} \tag{2}$$

$$\frac{f(\chi)}{f(Z_S)} = \frac{1+c\left[\exp(d\chi)-\exp(d\pi/2)\right]+e\ \cos^2\chi}{1+c\left[\exp(dZ_S)-\exp(d\pi/2)\right]+e\ \cos^2 Z_S} \tag{3}$$

where L is the sky luminance in an arbitrary sky element (cd/m²); LZ is the sky luminance at the zenith (cd/m²), Z is the zenith angle of a sky element (rad); ZS is the zenith angle of the sun (rad); χ is the scattering angle (degrees) (i.e. shortest angular distance between the sky point and the center of the sun)= arccos($\cos Z_S\cdot\ \cos Z+\ \sin Z_S\cdot\ \sin Z\cdot\ \cos|\phi-\phi_S|$), ϕ is the azimuth angle of the sky element (rad), ϕS is the azimuth angle of the sun (rad); *a*, *b*, *c*, *d* and *e* are adjustable coefficients

Both gradation and indicatrix functions are of six types. The combinations can form 36 skies but only 15 relevant types containing five clear, five partly cloudy and five overcast skies were adopted to be the standard skies. Table 1 summarizes the general features of the 15 CIE Standard Skies.

Table 1
Particulars for the 15 CIE Standard Skies.

No (code)	Gradation		Indicatrix			Sky description
	a	*b*	*c*	*d*	*e*	
1 (I1)	4	−0.7	0	−1	0	CIE standard overcast sky, steep luminance gradation towards zenith, azimuthal uniformity
2 (I2)	4	−0.7	2	−1.5	0.15	Overcast, with steep luminance gradation and slight brightening towards the sun
3 (II1)	1.1	−0.8	0	−1	0	Overcast, moderately graded with azimuthal uniformity
4 (II2)	1.1	−0.8	2	−1.5	0.15	Overcast, moderately graded and slight brightening towards the sun
5 (III1)	0	−1	0	−1	0	Sky of uniform luminance
6 (III2)	0	−1	2	−1.5	0.15	Partly cloudy sky, no gradation towards zenith, slight brightening towards the sun
7 (III3)	0	−1	5	−2.5	0.3	Partly cloudy sky, no gradation towards zenith, brighter circumsolar region
8 (III4)	0	−1	10	−3	0.45	Partly cloudy sky, no gradation towards zenith, distinct solar corona
9 (IV2)	−1	−0.55	2	−1.5	0.15	Partly cloudy, with the obscured sun
10 (IV3)	−1	−0.55	2	−2.5	0.3	Partly cloudy, with brighter circumsolar region
11 (IV4)	−1	−0.55	10	−3	0.45	White-blue sky with distinct solar corona
12 (V4)	−1	−0.32	10	−3	0.45	CIE standard clear sky, low luminance turbidity
13 (V5)	−1	−0.32	16	−3	0.3	CIE standard clear sky, polluted atmosphere
14 (VI5)	−1	−0.15	16	−3	0.3	Cloudless turbid sky with broad solar corona
15 (VI6)	−1	−0.15	24	−2.8	0.15	White-blue turbid sky with broad solar corona

3. Climatic variables

There are a number of daylight parameters for categorizing the 15 CIE Standard General Skies. The same standard sky type is assumed to have the identical well-defined sky luminance pattern and the corresponding climatic variables and indices would be within certain ranges. Such features can help the identification of sky patterns and complicated mathematical expressions to model the sky distributions are not required. The characteristics of the appropriate climatic parameters for classifying the 15 CIE Standard General Skies including L, L_Z/D_V, G_V/E_V, D_V/E_V, T_V and VSC are discussed as follows:

3.1. Sky luminance

Each CIE Standard General Sky is well-defined by sky luminance pattern which is the straightforward approach for sky identification. Sky luminance distributions particularly for the whole sky are seldom available for the sites under consideration or exist for very limited periods. The usual instrument for measuring sky luminance distribution is by means of a sky scanner [35]. There are however, several limitations regarding the accuracy of the recorded sky luminance readings. Firstly, the sensor head of the scanner rotates in altitude and azimuth to measure the luminance at 145 circular sky patches by scanning the sky hemisphere. Such a scanning pattern can avoid any double counting but it excludes certain regions of sky vault. Secondly, the measured data are considered discrete readings rather than continuous analytical expressions. Sky luminance between adjoining measurement points may vary considerably. Thirdly, each scanning period for the 145 points is about 4 min and the measurements are taken every 10 min. Great changes in sky luminance distributions may appear within each measurement. Additionally, for “out of range” measurements (points close to the sun location under non-overcast skies), an estimation of the sky luminance was made from a simple average of the luminance at nearby points. Such a conversion however, could introduce data distortion. Nonetheless, long-term systematic luminance measurements for the whole sky can provide sufficient data for analysis.

3.2. L_Z/D_V

The ratio L_Z/D_V is the original criterion to classify the sky luminance patterns into one of the 15 CIE Standard General Sky distributions [18]. The integration of the luminance of each sky patch over the whole sky vault gives D_V. Zenith is normal to the ground surface and D_V would be strongly related to L_Z. A good agreement (i.e. the zenith luminance is the main component contributing to D_V) does exist between these two daylight variables [36]. The 15 theoretical L_Z/D_V curves can distinguish quite well between skies at lower αs of 35° or less with clear-cut values from 0.1 to 0.41. Sky classification was conducted for high latitude regions during winter period (i.e. αs less than 35°) [37,38]. However, these 15 curves are not parallel and eventually they cross each other when $\alpha s > 35°$. This could give ambiguous results in sky classification for places of low latitudes [39].

3.3. G_v/E_v

The ratio G_V/E_V is often adopted to indicate the relative clearness of the atmosphere for sky categorization. In general, when the atmosphere is clear, a small fraction of the daylight illuminance is scattered, resulting in direct sunlight being predominant with a large G_V/E_V reading. Under overcast skies, a large portion of daylight illuminance is dispersed, indicating D_V is the main component with a small G_V/E_V value. The measurement of G_V is simple and straight. The recorded G_V/E_V should be more than zero and less than unity. Nonetheless, G_V/E_V may sometimes be ineffective to interpret the actual sky conditions. In an extreme case, one small cloud in a clear sky may keep the sun obstructed by slowly moving across the sky (i.e. small G_V/E_V). On the other hand, a small aperture in the clouds in an otherwise cloudy day may remain open to the sun for a long period (i.e. large G_V/E_V).

3.4. D_V/E_V

As the whole sky is considered, D_V should be an appropriate daylight variable to indicate the state of the sky. Basically, the measurement of D_V requires a shadow-ring to block the direct sunlight. The use of shadow-ring for recording D_V always obstructs a significant portion of the sky hemisphere. Correction must be applied to the measured D_V to obtain the true readings. Owing to the anisotropy of sky-diffuse component with its maximum being close to the sun, correction model considering anisotropic effects should be employed. High D_V/E_V values often appear in partly cloudy skies. For relative low D_V/E_V readings, they may denote either overcast or clear sky conditions. Once the three typical sky conditions (i.e. overcast, partly cloudy and clear) have been distinguished, D_V/E_V can be used to further differentiate the overcast and clear skies [32].

3.5. T_v

Sky contains air molecules, water vapor, dust and aerosols. The attenuation of luminous solar energy through atmosphere indicates the luminous turbidity (T_v), which is an appropriate index for elaborating the daylight climates and sky clearness under cloudless sky conditions. The mathematical expression for T_v is given as: [18,26]:

$$T_v = \frac{\ln(E_v/B_v)}{a_v m_v} \tag{4}$$

where B_V is the direct-beam daylight illuminance (lux), a_V is the luminous ideal extinction$=1/9.9+0.043\ m_v$ [40], m_V is the optical air mass$=1/\ \sin\ \alpha_S+0.50572(\alpha_S+6.07995)^{-1.6364}$ [41]

Under cloudless skies, T_V relates to the atmospheric transmittance in the direction of the direct sunlight to overall skylight efficiency [42]. When there is no Bv, T_V becomes infinite for overcast skies. It means that T_V cannot be used to single out individual overcast skies. However, it has been shown that T_V is a good parameter to differentiate between clean and polluted cloudless skies [43]. The typical T_V ranges are between 10 and 15 for partly cloudy skies and below 6.5 for clear days which can be adopted to interpret individual intermediate and cloudless sky conditions [32].

3.6. Vertical diffuse illuminance

With luminance distribution for the whole sky, daylight illuminance on various tilted surfaces such as vertical planes facing different orientations can be estimated by integrating the luminance distribution of the sky dome 'seen' by the surface [14]. Vertical sky component (VSC) is defined as the ratio of the vertical diffuse illuminance (D_{VT}) to the unobstructed horizontal diffuse illuminance (DV) available at the same point [44]. The sky-diffuse illuminance for the CIE Standard General Skies 1, 3 and 5 can be determined using double integrals. However, it is not possible to compute the exact sky-diffuse illuminance for other CIE skies particularly the non-overcast types. Applying numerical techniques, D_{VT} and DV can be expressed as [45,46]

$$D_V = \sum_{j=1}^{m}\sum_{i=1}^{n} L_{ij}\cos\ \alpha_i\ \sin\ \alpha_i\ \delta\alpha_i\ \delta\phi_j \tag{5}$$

$$D_{VT} = \sum_{j=1}^{m}\sum_{i=1}^{n} L_{ij}\cos^2\alpha_i\ \cos\ (\phi-\phi_{Nr})_i\delta\alpha_i\ \delta\phi_j \tag{6}$$

(For $0\le\alpha\le\pi/2,\ -\pi/2\le\phi-\phi_{Nr}\le\pi/2;=0$ otherwise)

where α is the altitude angle of a sky element (rad); and ϕ_{Nr} is the azimuth angle of the surface normal (rad)

Horizontal diffuse illuminance is not influenced by the azimuthal position of sky luminance patch. The VSC facing a

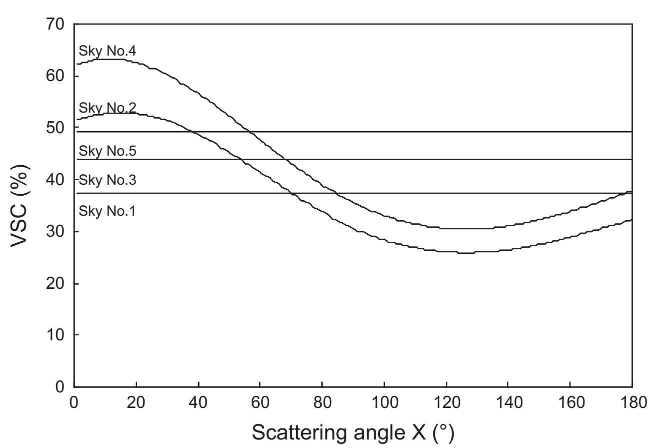


Fig. 1. VSC for the five unobstructed overcast skies (CIE Standard General Skies 1–5).

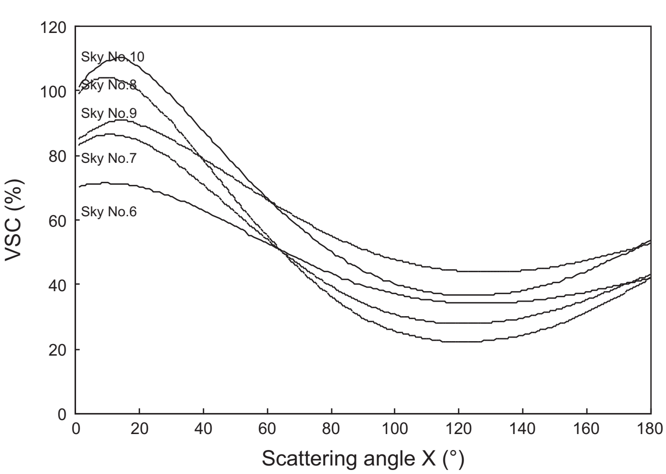


Fig. 2. VSC for the five unobstructed partly cloudy skies (CIE Standard General Skies 6–10).

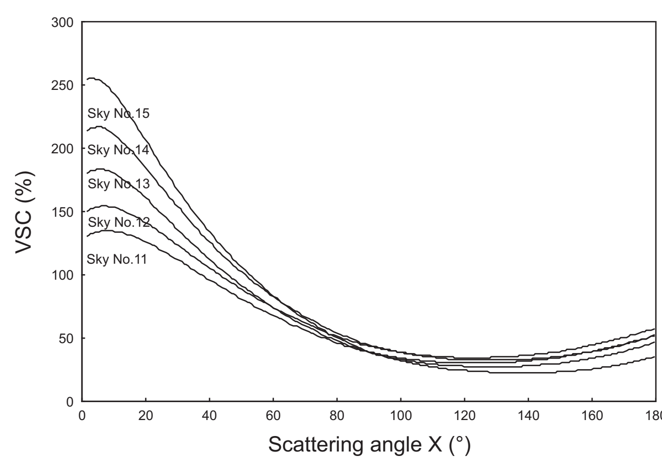


Fig. 3. VSC for the five unobstructed clear skies (CIE Standard General Skies 11–15).

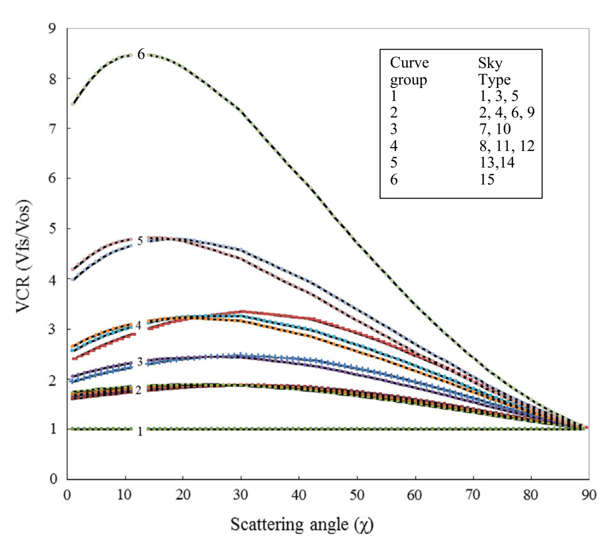


Fig. 4. Vertical component ratios (VCR) for various χ.

particular orientation for a given solar position under an individual CIE Standard General Sky has its own characteristics and accounts for a unique value. The scattering angle (χ) is the angular distance between a sky-element and the actual location of the solar. The sun position is always expressed by two solar angular coordinates namely zenith/altitude and azimuth angles. It indicates that a given χ can stand for many combinations of solar zenith/altitude and azimuth angles. For computing χ, the location of the sky elements is at zero altitude angle and azimuth angle of the window normal. Fig. 1 plots the χ against the VSC for the Standard General Skies 1–5 (the five overcast skies). For sky standards 1, 3 and 5 (i.e. dark overcast skies with azimuthal uniformity), the VSC is independent of χ. Constant VSC values for these three sky standards range between 40% and 50%. For Standard General Skies 2 and 4, they are slight brightening toward the sun and the VSC changes with χ. The VSC varies between 27% and 53% for Standard General Sky 2 and from 32 to 64% for Standard General Sky 4. It is interesting to note that the two curves do not cross each other. Similarly, the VSC at various χ for the Standard General Skies 6–10 (i.e. partly cloudy skies) and Standard General Skies 11–15

Table 2
The sky number in each of the curve groups.

Curve group number	1	2	3	4	5	6
Sky number	1, 3 and 5	2, 4, 6 and 9	7 and 10	8, 11 and 12	13 and 14	15

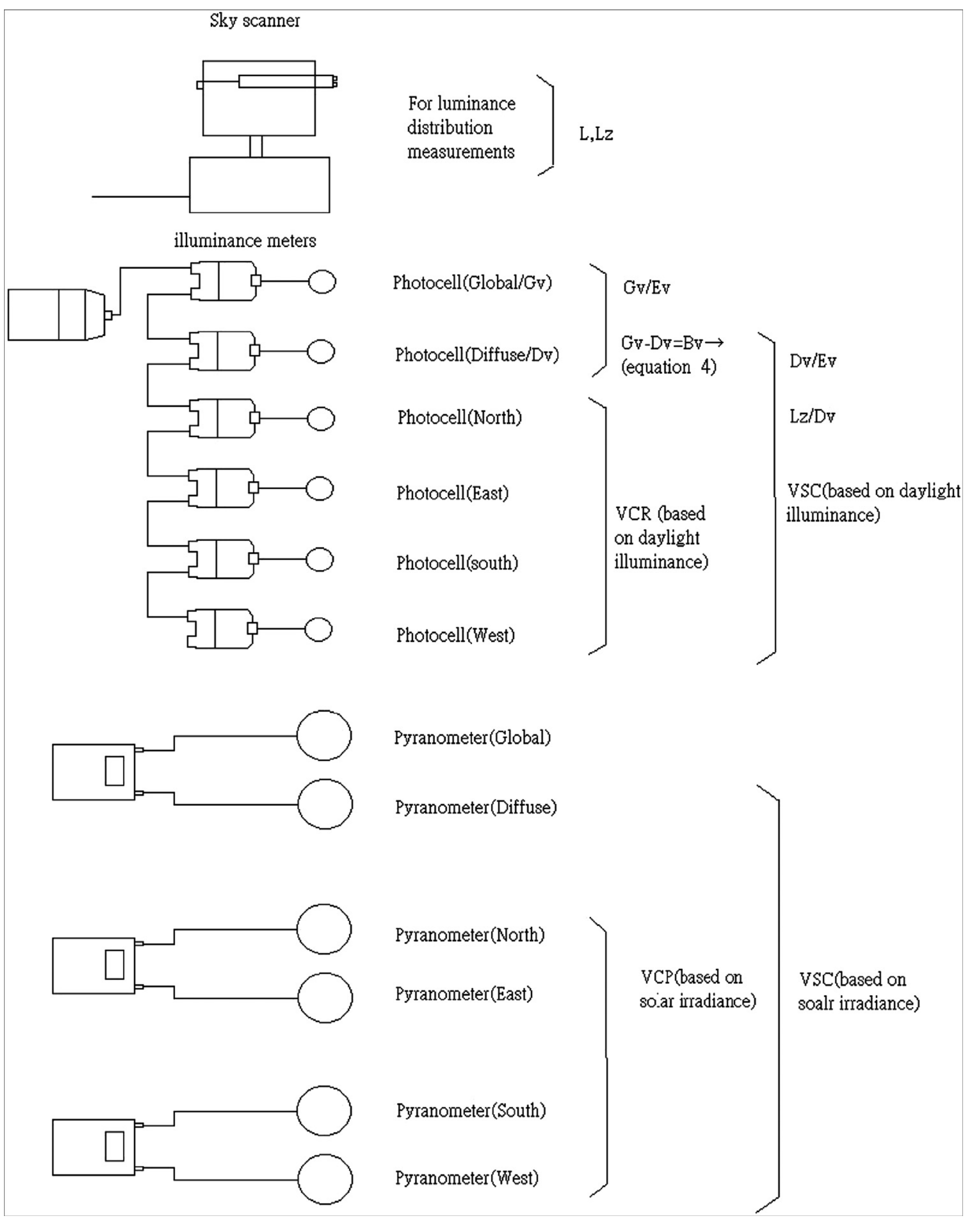


Fig. 5. The measuring mechanisms of the solar and daylight variables used for sky classification.

(clear skies) are presented in Figs. 2 and 3, respectively. Under non-overcast sky conditions, the VSC depends strongly on the sun position. Generally, peak VSC appears at low χ of around 10°. Then, the VSC drops with increasing χ up to about 100°. When χ is between 100° and 140°, VSC is at its minimum value. Then, VSC rises slightly with increasing χ. It can be observed that the curves intersect with one another at certain solar positions but a thorough analysis of Fig. 2 revealed that sky standards 7 and 10 are quite parallel and do not cross each other. Similar pattern can also be found for sky standards 6 and 9. As the cloud amount further reduces (i.e. clear skies), the solar corona effect becomes more substantial. Larger VSC values are resulted for the General Standard Skies 11–15 (i.e. clear skies). At small χ less than 45° the five curves are separate from each other. However, the curves converge and eventually they overlap at χ above 50°. Similar findings were also reported by Alshaibani [47]. Such features are important for sky categorization.

Under dark overcast skies with azimuthal uniformity (i.e. General Standard Skies 1, 3 and 5), the luminance distribution is symmetrical about the zenith and changes with the elevation above the horizon. It means that the vertical outdoor illuminance would be the same for all orientations. For non-overcast skies, very large sky luminance would occur near to the sun dropping rapidly with the angular distance from the solar, particularly for cloudless skies. As pointed out by Alshaibani [48], the ratio of the sky illuminance on a vertical surface facing the sun to that facing the opposite orientation (V_{fs}/V_{os}) for instance the vertical component facing south to that facing north can show some clear distinctions between groups of certain skies. Fig. 4 presents such vertical component ratios (VCR) under various χ which only refer to the vertical surface facing the sun (surface with the smallest χ) between 0° and 90°. Totally, six distinguish indicatrix categories with the V_{fs}/V_{os} ratios ranging from 1 to over 8 can be formed. Each category may contain 1–4 sky types that are summarized in Table 2 [48]. It indicates that ratios of vertical sky illuminance and VSC can be applied for the sky categorization. Fig. 5 presents the measuring mechanisms of the solar and daylight variables used for sky classification.

4. Sky classification approaches

Previously, several approaches were used for classifying the 15 CIE Standard General Skies [20,32,34]. The sky classification procedures with some modifications are elaborated as follows:

4.1. Sky luminance (Approach I)

Sky luminance distributions for the whole sky vault perhaps are the most appropriate data for sky classification. To identify the set of standard skies, the luminance distributions of individual sky standards were modeled using Eqs. 1–3 and compared with the scanned sky luminance readings. The modeled sky luminance should be initially normalized to the horizontal diffuse illuminance by multiplying all the luminance values with the normalization ratio (NR) as

$$NR = \frac{\sum L_{mea} \cos\alpha \sin\alpha \, d\alpha \, d\phi}{\sum l_{pred} \cos\alpha \sin\alpha \, d\alpha \, d\phi} \quad (7)$$

where L_{mea} is the measured sky point luminance (cd/m^2); l_{pred} is the predicted sky point luminance in relative form (dimensionless).

Once the integrated diffuse illuminance and l_{pred} at each sky point has been obtained, the predicted sky luminance (L_{pred}) which is the product of NR and l_{pred} can be easily computed. An alternative would be to divide all sky luminance readings by the corresponding L_Z, but this can cause huge measuring error when the sun is near to the zenith [24]. For low-latitude climates (e.g. Hong Kong) when the sun is frequently within a small angular distance from zenith, a normalization with respect to the D_V would, therefore, be more suitable. Once normalized, the performance of each standard sky luminance model was assessed by the root-mean-square error (RMSE):

$$\mathrm{RMSE} = \sqrt{\frac{1}{N}\sum\left(\frac{L_{pred}-L_{mea}}{L_{mea}}\right)^2} \quad (8)$$

where N is the number of readings (dimensionless).

The standard sky interpreted is the one with the lowest RMSE. The procedures are repeated for every measured luminance scan. Ultimately, the frequency of the identified 15 CIE General Standard Skies and the corresponding RMSE can be determined.

4.2. Appropriate daylight variables (Approach II)

The original criterion for classifying the sky luminance patterns into one of the 15 Standard General Skies is the L_Z/D_V which can characterize the momentary sky brightness. However, the L_Z/D_V theoretical curves for the 15 Standard skies are not parallel and they intersect with each other at the αS of higher than 35°. The global daylight components (G_V) of quite straight measurement procedures are appropriate data for classifying daylight climates. Direct-beam horizontal daylight (B_V) can be obtained by subtracting the corrected D_V from the corresponding G_V. The 15 CIE General Standard Skies can be categorized by such four horizontal daylight parameters. As proposed by Kittler and Darula [26], the pair $L_Z/D_V - G_V/E_V$ is an effective hybrid daylight-variable to identify the three typical sky conditions (i.e. overcast, partly cloudy and clear). There are no clear-cut values for $L_Z/D_V - G_V/E_V$ to represent different sky types. The $L_Z/D_V - G_V/E_V$ ranges for the categorization of the three typical skies using Hong Kong measured data were computed [43] and are shown in Table 3. To further distinguish between the five sky types under each of the typical skies (i.e. overcast, partly cloudy and clear), we proposed the criteria for the various parameters including L_Z/D_V, G_V/E_V, D_V/E_V and T_V and are summarized in Fig. 6 [32]. Two sky classification procedures using these daylight variables are adopted. When the data are measured at αS of 35° or below, the theoretical L_Z/D_V curves are used for categorizing all the 15 CIE General Standard Skies. The criteria for classifying standard skies are universal. For the data recorded at αS more than 35°, the procedures presented in Table 3 and Fig. 6 are applied [49]. The necessary data are the basic daylight parameters. L_Z is the 145th measurement point for the sky scanning. The global and diffuse outdoor illuminance on a horizontal surface can be used to compute the required daylight variables.

Table 3
The criteria for the classification of the 3 typical sky conditions based on the hybrid daylight parameter $L_Z/D_V - G_V/E_V$.

Sky conditions	Criteria
Overcast	$L_Z/D_V \geq 0.3$ and $G_V/E_V \leq 0.3$
Partly cloudy	$0.17 < L_Z/D_V < 0.3$ and $G_V/E_V \leq 0.3$ or $L_Z/D_V > 0.17$ and $0.3 < G_V/E_V < 0.5$
Clear	$L_Z/D_V \leq 0.17$ or $L_Z/D_V \geq 0.17$ and $G_V/E_V \geq 0.5$

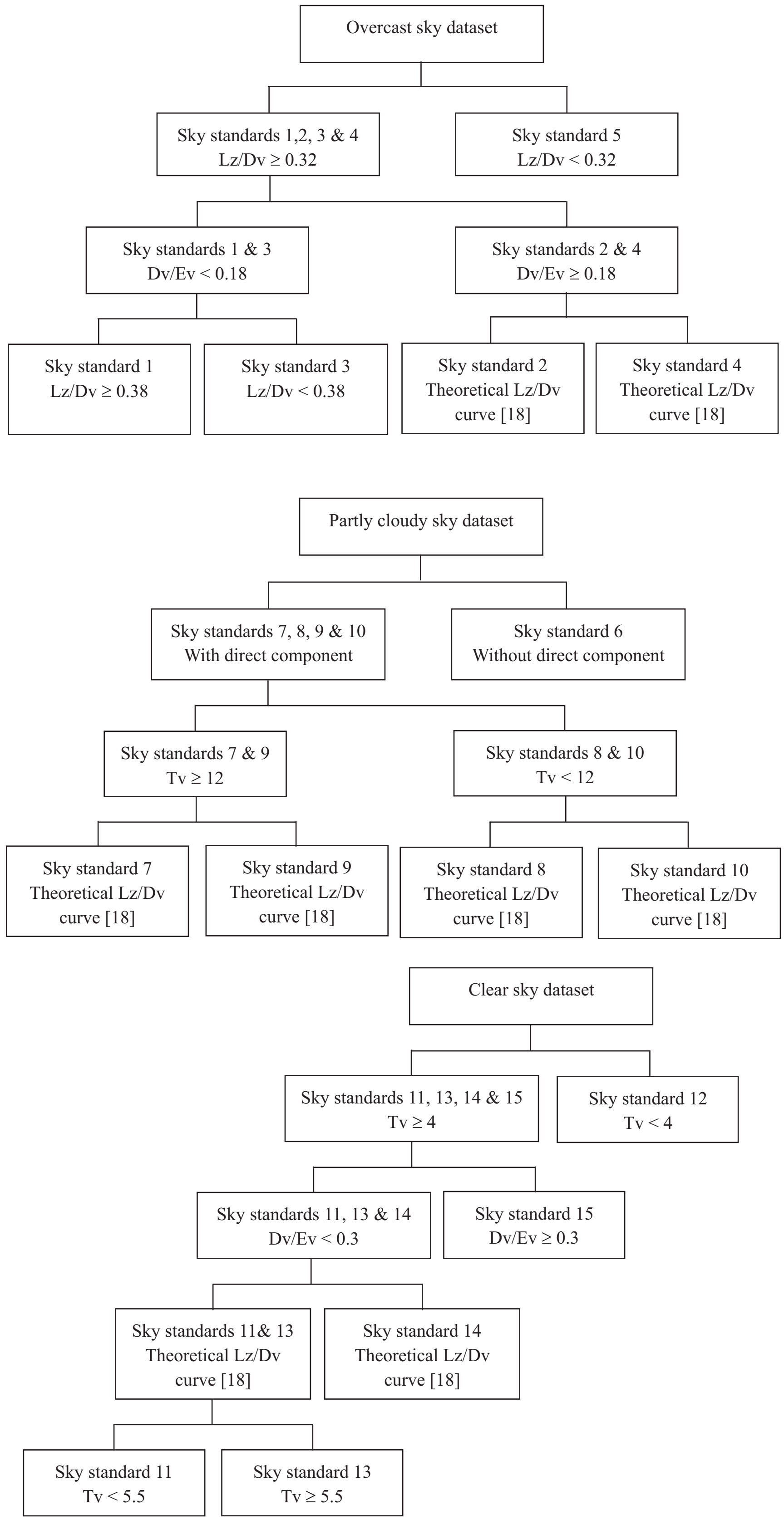


Fig. 6. The criteria for the classification of the 15 CIE Standard General Skies using the appropriate daylight indices.

4.3. Vertical sky illuminance (Approach III)/irradiance(Approach IV)

For sky classification, the VCR (V_{fs}/V_{os} ratios) from the measured vertical illuminance facing the four cardinal orientations (i.e. N, E, S and W) were determined and categorized into one of the six indicatrix groups (i.e. Fig. 4). Each indicatrix group contains only one to four sky types. Apart from indicatrix group 5, the VSCs for the sky types within a particular indicatrix group are parallel for all χ. It means that the sky type can further be identified by using VSC. For the indicatrix group 5 (Skies 13 and 14), only the VSC with the smallest χ (usually less than 45°) was used for sky classification. Daylight is the visible portion of solar radiation and both solar radiation and daylight illuminance have similar characteristics in nature. The same sky classification procedures can be applied to solar irradiance data which are more available than daylight illuminance [48] (Approach IV). The methodology is universal and only the measurements of the horizontal and two vertical sky-diffuse components are sufficient to identify the standard skies.

5. Sky classification and performance evaluation

The measurements of solar irradiance, daylight illuminance and sky luminance were made by a measuring station located at the City University of Hong Kong. All sensors were installed on the rooftop in a position relatively free from any external obstructions, and readily accessible for inspection, general cleaning and maintenance. The data collection started just before sunrise and finished after sunset every day. All data were measured approximately simultaneously in true solar time which facilitates the computations regarding solar geometry and the subsequent comparison of the data at other locations. Six pyranometers were used to carry out the measurements of global and diffuse irradiance on a horizontal surface and the global irradiance on the vertical planes facing the four cardinal orientations (i.e. north, east, south and west). The irradiance data were captured simultaneously twice per second, averaged over 10-min intervals and transmitted to the computers for storage. The daylight illuminance data namely the global and diffuse components on a horizontal surface, and vertical global illuminance facing north, east, south and west were measured by six illuminance meters (T-10M) manufactured and calibrated by Minolta of Japan. Similar record procedures as solar irradiance were adopted for daylight illuminance measurements. The sky luminance distributions are scanned using a sky scanner (EKO MS 300LR). It records the luminance at 145 points of sky by scanning the sky dome. The full view angle of the scanner is 11° allowing each sky patch to be treated as a point source with negligible error [50]. The important parts of the sky scanner are housed in a weatherproof casing for continuous outdoor operation. The data from the scanner are recorded on a microcomputer placed inside the laboratory on the top floor. To safeguard the sensor, the scanner does not record luminance data larger than 35 kcd/m² by using an automatic shutter. Details of the solar irradiance, daylight illuminance and sky luminance/radiance measurements can be found in our previous studies [20,35]. To eliminate spurious data and erroneous measurements due to the cosine effect of the sensors, proper quality-control tests were adopted. Details of the test procedures can be referred to our past work [31]. The 10-min data measured in 2004 (January to December) were employed for the analysis and the quality control tests were conducted. It is inevitable that there were some periods of missing data for various reasons such as instrumentation malfunction, power failure and senor calibration. Considerable efforts were made to obtain a continuous record of data. After the quality-control tests, around 15,000 data were retained for subsequent analysis. The six pyranometers, six illuminance meters and the sky scanner form a systematic measurement to collect the climatic variables for categorizing the standard skies. Through the stringent quality-controls tests, it indicates that the data recorded in Hong Kong have the representativeness for skies classification.

5.1. Sky classification

Accordingly, the categorizations of the 15 standard skies using the four methods were determined. Fig. 7 presents the results using the best-fitting sky luminance approach (Approach I). Large variations can be observed for individual sky types and a thorough analysis of the figure revealed that the frequency of overcast (Sky nos. 1–5) and clear (Sky nos. 11–15) skies was quite close. Totally,

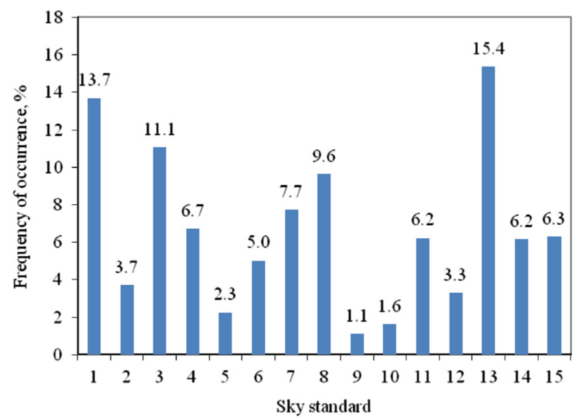


Fig. 7. Frequency of occurrence of the 15 CIE skies classified by sky luminance data (Approach I).

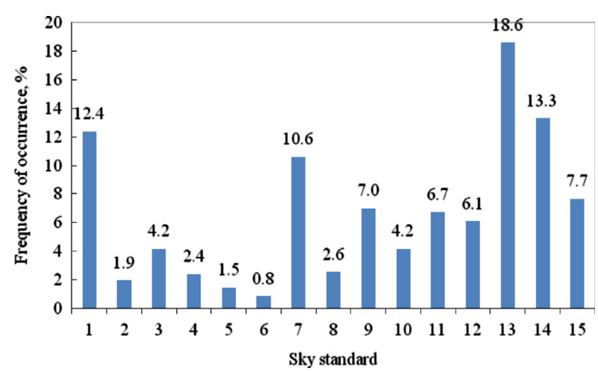


Fig. 8. Frequency of occurrence of the 15 CIE skies classified by appropriate daylight variables (Approach II).

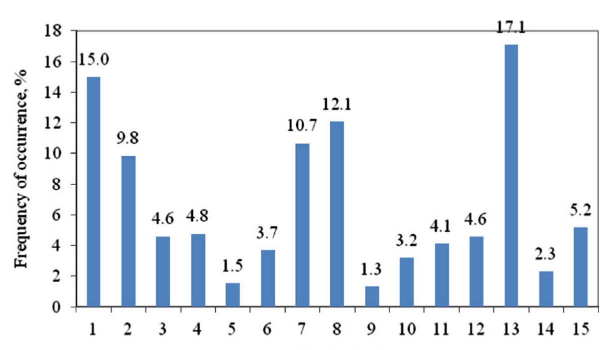


Fig. 9. Frequency of occurrence of the 15 CIE skies classified by VCR and VSC using daylight illuminance data (Approach III).

about 75% of the skies were categorized into overcast and clear conditions. The partly cloudy skies (Sky nos. 6–10) represent the remaining 25%. Sky nos. 1 and 3 dominate the overcast sky. Sky nos. 7 and 8 are the main sky patterns for the partly cloudy condition. For clear sky condition, it is matched by Sky no. 13. The findings are in good agreements with our previous work using data recorded between 1999 and 2005 [32]. Fig. 8 displays the frequency of occurrence of the 15 standard skies using the appropriate daylight variables (Approach II). The distribution is quite different. Based on the classification method, more than 50% skies were identified as clear state. Sky nos. 1, 7, 13 and 14 are the four most frequent standards representing 12.4, 10.6, 18.6 and 13.3%, respectively. Likewise, the frequency of occurrence of the 15 standard skies according to the VCR and VSC based on daylight illuminance (Approach III) and solar irradiance (Approach IV) are respectively plotted in Figs. 9 and 10. It can be seen that the two figures depict similar patterns. This is not surprising, given that daylight is the visible portion of solar radiation. Generally, the two figures show that the sky standards are quite evenly distributed in terms of the three typical sky types (i.e. overcast, partly cloudy and clear) under such categorizations. The majority of the overcast conditions are Sky nos. 1 and 2. Referring to partly cloudy conditions, Sky nos. 7 and 8 are the main sky type. For clear sky condition, Sky no. 13 has the largest frequency. Among all the sky classification approaches adopted, Sky no. 13 can be considered the most representative clear sky type from the CIE Standard Skies in Hong Kong ranging between 15.4 and 18.6%. This supports the argument that Hong Kong is currently infamous for its poor air quality and polluted conditions. All findings show that in Hong Kong Sky nos. 1 and 13 are respectively the main sky patterns for overcast and clear sky conditions which are consistent with previous studies [8,20,27,32,34,44,49,51].

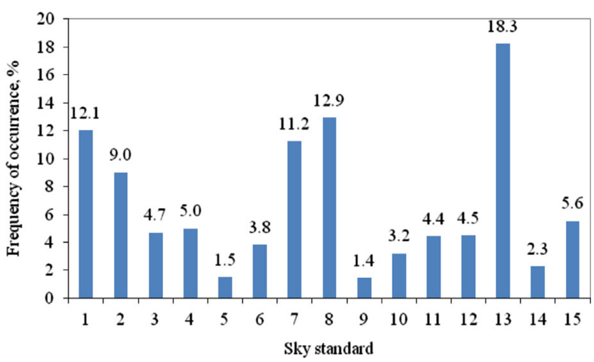


Fig. 10. Frequency of occurrence of the 15 CIE skies classified by VCR and VSC using solar irradiance data (Approach IV).

5.2. Performance evaluation

For the development of active solar applications, passive solar building designs and daylighting schemes, vertical global values are always required. To evaluate whether the skies are correctly identified, the global components for the four (i.e. N, E, S and W) cardinal vertical surfaces were modeled based on the sky types classified by the various approaches. The daylight illuminance incident on a vertical surface (G_{VT}) is the sum of direct-beam (B_{VT}), sky-diffuse (D_{VT}) and ground-reflected (R_{VT}) components. Mathematically, it can be expressed as

$$G_{VT} = B_{VT} + D_{VT} + R_{VT} \tag{9}$$

Calculation of B_{VT} is quite simple, given the position of the sun and orientation of the surface. For estimating the R_{VT}, it is assumed that

Table 4
Summary of %MBE and %RMSE for vertical daylight illuminance based on the skies classified by Approach I.

	Jan	Feb	Mar	Apr	May	Jun	Jul	Aug	Sep	Oct	Nov	Dec	Year
North													
% MBE	−12	−7.8	−8.3	−10.2	−9.8	−5.2	−10.2	−17.1	−18.5	−17	−18.8	−21.1	−12.4
% RMSE	13.3	13	14.9	17.1	16.7	13.2	17.4	22.8	21.9	19.3	20.3	22.1	19.7
East													
% MBE	−3.8	−3.2	−0.4	4.2	3.5	4.9	4.6	1.8	−0.7	0.5	−5.2	−8	1
% RMSE	11.8	11.7	12.4	15	15.2	14.6	16.9	14.3	12.7	12	14.4	13.3	14
South													
% MBE	1.4	−1.3	−3.2	−7.5	−14.9	−18.1	−19.7	−14.8	−5.3	−0.8	1.6	−0.8	−6.3
% RMSE	5.4	9.3	11	15.3	19	20.3	22.9	20	13.2	8.3	8.6	8.3	15.8
West													
% MBE	−18.7	−10.9	−7.5	−2.6	0.4	2	−2.4	−2.6	−6	−10.7	−16.8	−22.1	−6
% RMSE	23.8	18.5	16.2	12.2	12.3	12.4	12.6	13.2	15.5	16.6	21.8	25.3	15.6

Table 5
Summary of %MBE and %RMSE for vertical daylight illuminance based on the skies classified by Approach II.

	Jan	Feb	Mar	Apr	May	Jun	Jul	Aug	Sep	Oct	Nov	Dec	Year
North													
% MBE	−7.7	−6.8	−7.6	−8.9	−6.7	−1.8	−8.2	−13.7	−14.5	−12.2	−16	−19	−9.7
% RMSE	13.3	15.8	16.7	17.5	16	12.9	17.4	20.5	20.7	17.1	19.3	21.6	19.2
East													
% MBE	−0.5	−0.2	3.8	8.6	7	8.2	7.4	5.5	1.3	2.2	−3.5	−8.2	3.9
% RMSE	12.4	14.7	19.3	23.7	21.2	19.9	23.7	20.2	14.2	12.8	15	13.7	18.8
South													
% MBE	2.9	3.5	3.2	−3	−11.8	−14.9	−18.4	−10.9	−1.3	1.3	3.8	−0.5	−3.1
% RMSE	5.7	13.8	15.1	16.5	18.3	18.3	23	18.4	15	9.5	11.3	11	16.3
West													
% MBE	−18.1	−8.2	−4.3	1.1	4.7	5.9	0.6	1.6	−1.3	−8.4	−15.4	−21.8	−2.8
% RMSE	24	17.6	16.2	17.7	18.2	18.1	18.4	16.9	16.6	15.4	20.9	25.3	17.9

vertical surface receives half of the total illuminance reflected isotropically from the ground and ignoring the inter-reflection between the vertical and the ground surfaces which is a second-order effect of lesser importance. Hence, B_{VT} and R_{VT} can be expressed as follows:

$$B_{VT} = (B_V / \sin \alpha_S) \cos \alpha_S \cos(\phi_S - \phi_{Nr}) \quad (10)$$

$$R_{VT} = \rho G_V / 2 \quad (11)$$

where ρ is the ground reflectance (dimensionless)

For determining R_{VT}, a common average ρ value of 0.2 is applied. Likewise, the same calculation procedures can be employed to determine the sky-diffuse solar irradiance on a vertical plane (I_{VT}). The performance was assessed by two widely used statistics, mean-bias-error (MBE), a measure of the underlying trend, and root-mean-square-error (RMSE), an indication of data scattering.

Table 4 presents the MBE and RMSE results for the vertical daylight illuminance facing the four principle orientations in all 12 months and the whole year using the Approach I (i.e. sky luminance distributions). The daylight illuminance data for north-facing surface are under-estimated for all months with an annual MBE of −12.4%. For other vertical planes, the MBEs vary between an under-estimation of 22.1% in December for west-facing surface to an over-estimation of 4.9% in July for east-facing surface. The RMSEs range from 5.4% in January to 22.9% in July appearing both at south-facing surface. The annual RMSEs for the four vertical surfaces are below 20%. Likewise, the MBEs and RMSEs for the vertical daylight illuminance based on Approach II (i.e. appropriate daylight variables) are summarized in Table 5. Again, daylight illuminance data are under-estimated in all months for north-facing surface. For the whole year, the MBEs are −9.7%, 3.9%, −3.1% and −2.8% for north, east-, south- and west-facing planes. The peak monthly RMSE of 25.3% appears in December for west-facing surface. The annual RMSEs do not differ in great deal, ranging from 16.3 and 19.2%. The MBEs and RMSEs for the vertical daylight illuminance using the Approach III (sky classified by VCR and VSC using daylight illuminance data) and Approach IV (sky classification by VCR and VSC using solar irradiance data) are listed respectively in Tables 6 and 7. In general, they have similar annual RMSE pattern. The RMSEs for the whole year based on Approach III are 14.6, 20.6, 14.1 and 20.9% for north-, east-, south- and west-facing surfaces, respectively. Using Approach IV, the annual RMSEs are 0.2–4.2% more than those based on Approach III.

In view of the fact that solar irradiance and daylight illuminance have similar characteristics in nature, the methods for daylight illuminance prediction can also be employed in solar irradiance calculations [52]. Similarly, the monthly and annually MBEs and RMSEs for the vertical solar irradiance facing the four cardinal directions based on the four approaches were computed and are summarized in Tables 8–11. Generally, the four approaches have quite good performance in terms of the annual RMSEs. The maximum annual RMSE is not more than 21%. The results also show that the Approach III (Table 10) predicts the solar irradiance the best with the lowest annual RMSE of 9.7% appearing at east-facing surface.

6. Conclusions

Various approaches for sky classification were elaborated and reviewed. The strengths and limitations of the meteorological parameters including luminance distribution for the whole sky including zenith luminance, global, direct-beam and sky-diffuse illuminance on

Table 6
Summary of %MBE and %RMSE for vertical daylight illuminance based on the skies classified by Approach III.

	Jan	Feb	Mar	Apr	May	Jun	Jul	Aug	Sep	Oct	Nov	Dec	Year
North													
% MBE	1.1	−2	−1.1	−3.1	−2.9	0.1	−3.3	−8.7	−6	−5	−6.2	−3.9	−4.5
% RMSE	6.6	9	9.4	12.8	16.5	15	18.9	20	11.7	9.4	9.6	6.3	14.6
East													
% MBE	9	2	6.3	9.3	6.9	8.5	6.2	7	7.1	10.8	4.2	6.2	7
% RMSE	16.4	15	15.2	17.8	14.9	18.2	17.9	24	23.5	28.1	24.4	22.7	20.6
South													
% MBE	9.9	4.4	3.6	−2	−9	−6	−7.1	−8.3	−0.4	6.1	9.6	9.8	−0.9
% RMSE	11.8	14.9	9.8	12.4	14.3	8.5	10.9	17.3	15.5	14.8	20.5	13.7	14.1
West													
% MBE	3.5	−2.5	4.1	8.9	8.9	8.8	5.2	6	4.6	−0.9	−10.2	−9.9	2.7
% RMSE	26.8	18.5	17.5	20.4	17.7	18.8	20.4	24	23.4	23.3	23.4	17.2	20.9

Table 7
Summary of %MBE and %RMSE for vertical daylight illuminance based on the skies classified by Approach IV.

	Jan	Feb	Mar	Apr	May	Jun	Jul	Aug	Sep	Oct	Nov	Dec	Year
North													
% MBE	25.8	6.5	3.1	0.5	−0.2	2.4	−0.7	−4.8	−2.7	−0.6	−2.6	−1.5	0.1
% RMSE	31.3	17.5	15.6	11.9	11.1	15.7	14.9	16.2	15.5	14.8	13.2	10.5	14.8
East													
% MBE	21.1	7.1	9.2	11.9	6.6	11.6	10.4	4.7	0.4	3.1	−3.2	−4.3	6
% RMSE	25	22.5	26.6	26	19.8	28.4	25.6	22.6	21.6	19.6	19.2	17.2	23.4
South													
% MBE	3.1	3	6.2	2.3	−3.7	−6.1	−6.8	−3.9	0	−3.8	−8.1	−9.5	−2.5
% RMSE	10.9	19.8	12.2	11.8	9.8	13.7	13.6	14.1	16.2	13.4	28.3	27	15.9
West													
% MBE	−2.7	−3.4	1.5	5.9	7.1	6.5	2.6	3.4	1.1	−11.1	−17.6	−19.1	−1.2
% RMSE	10.3	27	22.6	26.7	26.9	23.2	23.2	26	23.8	23.1	29.8	26.5	25.1

Table 8
Summary of %MBE and %RMSE for vertical solar irradiance based on the skies classified by Approach I.

	Jan	Feb	Mar	Apr	May	Jun	Jul	Aug	Sep	Oct	Nov	Dec	Year
North													
% MBE	−11.2	1.1	3.7	1.1	2.2	5.7	5.6	−0.7	−5.8	−7.7	−13	−15.5	−1
% RMSE	14.6	13.6	18.5	15	15.7	17.4	18	16.1	16.4	14.7	16.4	17.9	16.3
East													
% MBE	−9	3.2	3.6	5.4	3	4.6	4.7	2.9	1.9	−3	−8.6	−12	1.6
% RMSE	13.7	12.3	12.8	17.6	17.7	19.6	21.7	21.7	20	11.2	15.1	16.9	17.5
South													
% MBE	−1.1	4.1	−1.1	−8	−2.9	−3.5	−4.6	−5.5	−2.7	−4.7	−3.1	−3.8	−3.4
% RMSE	9.4	22.6	18.3	17.8	16.6	16.6	17.1	19.7	20.6	12.2	13.7	15.2	17.6
West													
% MBE	−14.3	−0.2	−0.9	2.5	2.9	4.1	2.1	1.5	−4.3	−8.1	−13.3	−16.9	−1.6
% RMSE	19.7	15.2	15.2	19.8	17.5	17.1	18.6	18.6	15.2	11.9	16.5	19.8	16.8

Table 9
Summary of %MBE and %RMSE for vertical solar irradiance based on the skies classified by Approach II.

	Jan	Feb	Mar	Apr	May	Jun	Jul	Aug	Sep	Oct	Nov	Dec	Year
North													
% MBE	−6.1	2.2	4.3	1.7	4.7	8.2	7.1	2.2	−1.4	−2.7	−10.1	−13.3	1.5
% RMSE	14.1	15.8	22.1	17.4	17.8	18.7	19.6	17	18	14.3	16	17.1	17.8
East													
% MBE	−5.5	5.3	5.2	8.5	5.3	6.6	5.9	4.7	4.4	0.3	−6.4	−11.5	3.7
% RMSE	12.9	16.6	16.8	21.9	20.7	20.6	22.2	22	19.4	12.5	14.8	16.3	19
South													
% MBE	−0.1	7.8	1.2	−5.1	−0.2	−0.5	−3.2	−3	0.3	−2.6	−0.7	−2.6	−0.9
% RMSE	8.6	22.1	15.9	18.8	19.5	18.5	19.5	20	20.3	11.7	13.1	18.8	18
West													
% MBE	−12.4	1.6	0.3	4	7.3	6.7	3.9	4.4	0.6	−4.8	−11.1	−16.1	1
% RMSE	18	16	16.4	21.6	23.4	19.2	19.5	20.8	17	11.5	15.8	18.9	18.4

Table 10
Summary of %MBE and %RMSE for vertical solar irradiance based on the skies classified by Approach III.

	Jan	Feb	Mar	Apr	May	Jun	Jul	Aug	Sep	Oct	Nov	Dec	Year
North													
% MBE	1	−2	−1	−3.4	−4.1	−3.2	−5.5	−9.4	−8.1	−7.2	−8.3	−5.3	−5.2
% RMSE	6.3	8.6	9	12.6	12.6	13.9	18	19.9	15.6	13.5	12.9	8.7	14.1
East													
% MBE	2.5	−2.2	0.1	1.6	0.4	1.4	−0.2	−1.6	−2.6	−2	−6.3	−6.7	−1.2
% RMSE	6.3	11.2	6.2	6.7	9.1	9.2	9.2	11.8	10.2	9.9	12.6	11.3	9.7
South													
% MBE	1.1	−2.1	−2.6	−4.3	−7.4	−9.9	−10.5	−9.8	−6.5	−5.3	−7.2	−7.5	−6.5
% RMSE	5.1	10.9	8.2	11.5	11.1	13.8	15.9	16.7	14.6	12.2	13.4	11.7	13.1
West													
% MBE	−8.3	−6.5	−2.9	0.5	0.4	0.8	−3	−3.6	−5.3	−9.6	−16.1	−15.9	−5
% RMSE	10.5	14	7.6	8	6.8	8.3	11.7	13.9	13.3	15.9	22.4	20.2	12.9

Table 11
Summary of %MBE and %RMSE for vertical solar irradiance based on the skies classified by Approach IV.

	Jan	Feb	Mar	Apr	May	Jun	Jul	Aug	Sep	Oct	Nov	Dec	Year
North													
% MBE	2.7	7.5	8.6	6.4	15.3	9.4	10.2	4.8	4.2	3	−4.1	−2	5.9
% RMSE	9.2	13.1	15.1	15	16	18	18.3	16	16.7	13	12.6	9.9	15.5
East													
% MBE	5.1	9.7	8.1	9.4	16.5	8.8	7.2	9.9	13.7	8.5	2.5	2.1	8.6
% RMSE	10.6	20.7	13.7	17.4	22.3	20.9	22.6	23.8	28.9	17.6	14.7	15.2	20.7
South													
% MBE	13.1	11.3	6.4	−0.3	10.4	3.2	3.2	2.7	4.3	5.2	5.5	6.5	4.9
% RMSE	17.1	21	13.3	13.1	14	13.9	14.8	17.5	16.8	13.2	14	14.4	15.2
West													
% MBE	−3	3.8	5.5	10.6	18.4	10.3	10.7	9	4.7	1.1	−6.1	−5.7	5.4
% RMSE	14.3	16.2	13.9	22.5	21.5	20.2	20.8	18.6	16.9	14.6	13.7	11.6	18.1

a horizontal surface and vertical sky illuminance, and horizontal and vertical solar irradiance data for sky categorization were elaborated. Totally, four sky classification approaches with some modifications were proposed. Ten-minute solar irradiance and daylight illuminance data measured in 2004 were used for the study. The frequency of occurrence of the complete set of the 15 Standard General Skies was determined accordingly. Sky nos. 1 and 13 dominated respectively the overcast and clear conditions. For partly cloudy conditions, sky no. 8 is the main sky pattern based on Approaches I, III and IV. To evaluate whether the skies are correctly identified, the global solar irradiance and daylight illuminance for the four cardinal vertical surfaces were modeled based on the classified sky types. The performance was assessed in terms of mean-bias-error (MBE) and root-mean-square-error (RMSE). In general, the predicated vertical global components were in good agreements with those measured values. The peak annual RMSEs were 20.7 and 25.1% for solar irradiance and daylight illuminance, respectively. The findings support that once the skies have been correctly classified, good quality solar irradiance and daylight illuminance data on titled surfaces facing different directions can be estimated for subsequent analysis.

Acknowledgments

The work described in this paper was fully supported by a Competitive Earmarked Research Grant from the Research Grants Council of the Hong Kong Special Administrative Region, China [Project no. 9041470 (CityU 117209)].

References

[1] Quesada G, Rousse D, Dutil Y, Badache M, Halle S. A comprehensive review of solar facades. Transparent and translucent solar facades. Renew Sustain Energy Rev 2012;16(5):2643–51.
[2] Braun P, Ruther R. The role of grid-connected, building-integrated photovoltaic generation in commercial building energy and power loads in a warm and sunny climate. Energy Convers Manage 2010;51(12):2457–66.
[3] Serra R. Chapter 6-Daylighting. Renew Sustain Energy Rev 1998;2(1-2):115–55.
[4] Ma ZJ, Wang SW. Building energy research in Hong Kong: a review. Renew Sustain Energy Rev 2009;13(8):1870–83.
[5] Linhart F, Wittkopf SK, Scartezzini J-L. Performance of anidolic daylighting systems in tropical climates – parametric studies for identification of main influencing factors. Sol Energy 2010;84(7):1085–94.
[6] Singh MC, Garg SN. Illuminance estimation and daylighting energy savings for Indian regions. Renew Energy 2010;35(3):703–11.
[7] Markou MT, Bartzokas A, Kambezidis HD. Generation of daylight reference years for two European cities with different climate: Athens, Greece and Bratislava, Slovakia. Atmos Res 2007;86(3-4):315–29 (2007).
[8] Wong SL, Wan KKW, Li DHW, Lam JC. Generation of typical weather years with identified standard skies for Hong Kong. Build Environ 2012;56:321–8.
[9] Okogbue EC, Adedokun AA, Holmgren B. Hourly and daily clearness index and diffuse fraction at a tropical station, Ile-Ife, Nigeria. Int J Climatol 2009 2009;29(8):1035–47.
[10] Markou MT, Bartzokas A, Kambezidis HD. Daylight climatology in Athens, Greece: types of diurnal variation of illuminance levels. Int J Climatol 2009;29(14):2137–45.
[11] Singh HN, Tiwari GN. Evaluation of cloudiness/haziness factor for composite climate. Energy 2005;30(9):1589–601.
[12] Wen CC, Yeh HH. Comparative influences of airborne pollutants and meteorological parameters on atmospheric visibility and turbidity. Atmos Res 2009;96(4):496–509.
[13] Li DHW, Lam JC. Predicting solar irradiance on inclined surfaces using sky radiance data. Energy Convers Manage 2004;45(11–12):1771–83.
[14] Li DHW, Lau CCS, Lam JC. Predicting daylight illuminance on inclined surfaces using sky luminance data. Energy 2005;30(9):1649–65.
[15] Darula S, Kittler R. Sunshine duration and daily courses of illuminance in 5Bratislava. Int J Climatol 2004;24(14):1777–83.
[16] Li DHW, Lam JC. An Analysis of Climatic Parameters and Sky Condition Classification. Build Environ 2001;36(4):435–45.
[17] ISO, 15469:2004(E)/CIE S 011/E:2003. Spatial distribution of daylight – CIE Standard General Sky. ISO, Geneva, 2004.
[18] Kittler R, Darula S, Perez RA. Set of standard skies. Polygrafia: Bratislava; 1998.
[19] Janjai S, Plaon P. Estimation of sky luminance in the tropics using artificial neural networks: modeling and performance comparison with the CIE model. Appl Energy 2011;88(3):840–7.
[20] Li DHW, Lau CCS, Lam JC. A study of 15 sky luminance patterns against Hong Kong data. Archit Sci Rev 2003;46(1):61–8.
[21] Tregenza PR. Standard skies for maritime climates. Light Res Technol 1999;31(3):97–106.
[22] Wittkopf SK, Soon LK. Analysing sky luminance scans and predicting frequent sky patterns in Singapore. Light Res Technol 2007;39(1):31–51.
[23] Chirarattananon S, Chaiwiwatworakul P. Distributions of sky luminance and radiance of North Bangkok under standard distributions. Renew Energy 2007;32(8):1328–45.
[24] Tregenza PR. Analysing sky luminance scans to obtain frequency distributions of CIE Standard General Skies. Light Res Technol 2004;36(4):271–81.
[25] Soler A, Robledo L. Investigation of the overcast skies luminance distribution using 35 sensors fixed on a dome. Energy Convers Manage 2005;46(17):2739–47.
[26] Kittler R, Darula S. Parametric definition of the daylight climate. Renew Energy 2002;26(2):177–87.
[27] Li DHW, Lau CCS, Lam JC. Overcast sky conditions and luminance distribution in Hong Kong. Build Environ 2004;39(1):101–8.
[28] Li DHW, Lau CCS, Lam JC. Standard skies classification using common climatic parameters. J Sol Energy Eng 2004;126(3):957–64.
[29] Younes S, Muneer T. Clear-sky classification procedures and models using a world-wide data-base. Appl Energy 2007;84(6):623–45.
[30] JanJai S, Masiri I, Nunez M, Laksanaboonsong J. Modeling sky luminance using satellite data to classify sky conditions. Build Environ 2008;43(12):2059–73.
[31] Li DHW, Tang HL, Cheung KL, Lee EWM, Cheng CCK. Sensitivity analysis of climatic parameters for sky classification. Theor Appl Climatol 2011;105(3-4):297–309.
[32] Li DHW, Tang HL. Standard skies classification in Hong Kong. J Atmos Sol Terr Phys 2008;70(8–9):1222–30.
[33] Li DHW, Tang HL, Lee EWM, Muneer T. Classification of CIE standard skies using probabilistic neural network. Int J Climatol 2010;30(2):305–15.
[34] Li DHW, Cheung KL, Tang HL, Cheng CCK. Identifying CIE Standard Skies using vertical sky component. J Atmos Sol-Terr Phys 2011;73(13):1861–7.
[35] Li DHW, Lam JC, Lau CCS. A study of solar radiation daylight illuminance and sky luminance data measurements for Hong Kong. Archit Sci Rev 2002;45(1):21–30.
[36] Li DHW, Lam JC. An analysis of all-sky zenith luminance data for Hong Kong. Build Environ 2003;38(5):739–44.
[37] Markou MT, Kambezidis HD, Bartzokas A, Katsoulis BD, Muneer T. Sky type classification in Central England during winter. Energy 2005;30(9):1667–74.
[38] Bartzokas A, Darula S, Kambezidis HD, Kittler R. Sky luminance distribution in Central Europe and the Mediterranean area during the winter period. J Atmos Sol-Terr Phys 2003;65(1):113–9.
[39] Bartzokas A, Kambezidis HD, Darula S, Kittler R. Comparison between winter and summer sky-luminance distribution in Central Europe and in the Eastern Mediterranean. J Atmos Sol Terr Phys 2005;67(7):709–18.
[40] Navvab M, Karayel M, Ne'eman E, Selkovitz S. Analysis of atmospheric turbidity for daylight calculations. Energy Build 1984;6(2-4):293–303.
[41] Kasten F, Young AT. Revised optical air mass tables and approximation formula. Appl Opt 1989;28(22):4735–8.
[42] Darula S, Kittler R. New trends in daylight theory based on the new ISO/CIE sky standard. Zenith luminance formula verified by measurement data under cloudless skies. Build Res J 2005;53(1):9–31.
[43] Li DHW, Lau CCS. An analysis of non-overcast sky luminance models against Hong Kong data. J Sol Energy Eng 2007;129(4):486–93.
[44] Ng E, Cheng V, Gadi A, Mu J, Lee M, Gadi A. Defining standard skies for Hong Kong. Build Environ 2007;42(2):866–76.
[45] Li D.H.W., Lam T.N.T., Lam J.C. Average daylight factor under various skies and external environments. In: Proceedings of the fifth international conference on solar radiation and daylighting, 10–11 August 2011, Brno University of Technology, Czech Republic, pp.174–9.
[46] Li D.H.W., Lam T.N.T., Wu T.K.K.. Estimation of average daylight factor under obstructed CIE Standard General Skies. Light Res Technol 2014, http://dx.doi.org/10.1177/1477153512453578, in press
[47] Alshaibani K. Determination of CIE Standard General Sky from horizontal and vertical illuminance/irradiance. World Renewable Energy Congress X and Exhibition (WRECX), 19–25 July 2008, Glasgow-Scotland.
[48] Alshaibani K. Finding frequency distributions of CIE Standard General Skies from sky illuminance or irradiance. Light Res Technol 2011;43(4):487–95.
[49] Li DHW, Chau NTC, Wan KKW. Predicting daylight illuminance and solar irradiance on vertical surfaces based on classified standard skies. Energy 2013;2013:252–8.
[50] Tregenza P.R. Subdivision of the sky hemisphere for luminance measurements. Light Res Technol 19(1):13–14.
[51] Li DHW, Lau CCS, Lam JC. Evaluation of overcast-sky luminance models against measured Hong Kong data. Appl Energy 2001;70(4):321–31.
[52] Li DHW, Lam JC. Evaluation of slope irradiance and illuminance models against measured Hong Kong data. Build Environ 2000;35(6):501–9.